

Comparison of Measured and Predicted Inductance per Cell for a Travelling Wave Kicker Magnet

M.J. Barnes, G.D. Wait, TRIUMF

Abstract

Many present day kicker magnets must have a relatively short field rise time, and low flat-top and post-pulse ripple. In order to design the electrical circuit for a kicker magnet with the required specifications for field quality, it is necessary to quantify the effect of end-fields on the inductance distribution throughout the travelling wave kicker magnet. This paper presents the results of an electromagnetic analysis of a relatively short, 10 cell, prototype travelling wave kicker magnet using a three dimensional code capable of modelling eddy-currents: in order to verify the predictions, inductance measurements are also presented.

1 INTRODUCTION

As part of the Canadian contribution to CERN LHC, TRIUMF is assisting with the design of the injection system[1, 2]. 3D simulations of the LHC kicker magnets will be carried out: these simulations will permit inductance per cell to be calculated, and will include end effects. In order to prove the integrity of the 3D software, for simulating a kicker magnet, the code has been used to model an existing TRIUMF kicker magnet for which measurement data exists.

As part of the KAON Factory Project Definition Study a prototype kicker magnet, based on the design of those of CERN PS Division[3] was built at TRIUMF[4]. This kicker is of the transmission line type; it consists of ferrite C-cores sandwiched between high-voltage (HV) capacitance plates. The kicker has a ground conductor closing the aperture, which has the effect of both improving the magnetic field uniformity and minimising magnet fill-time. The kicker is a 10 cell magnet with a characteristic impedance of 30Ω .

The characteristic impedance (Z_0) of a cell of a transmission line kicker magnet is given by: $Z_0 = \sqrt{L/C}$, where L and C are the inductance and capacitance per cell of the kicker magnet, respectively. Impedance mismatches result in distortion of the current pulse, and therefore of the field in the kicker magnet[5]. Ripple of the field in the kicker magnet may result in an increase in beam injection losses.

2 MEASUREMENTS

In order to determine self-inductance per cell of the prototype kicker magnet, the kicker was driven with a pulse with a 30 ns rise time. Fig. 1 shows the propagation of

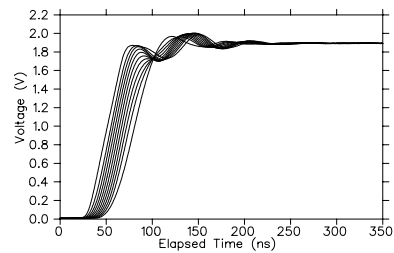


Figure 1: Pulse propagation through the prototype kicker

the pulse through each of the 10 cells of the kicker. A high impedance low-capacitance probe was used for measuring voltage on each of the HV capacitance plates. The kicker was driven from a 29Ω source and terminated with a $31.35\Omega(\pm 0.2\%)$ resistor (R_{out}) for this measurement. The ‘flat-top’ oscillations in Fig. 1 are damped out by an elapsed time of approximately 300 ns. The dimensions of the ferrite of a cell were chosen such that the field in the ferrite is below the knee of its B-H curve, at the design current of 1 kA. In addition the reluctance of the magnetic-circuit of a cell is dominated by the reluctance of the aperture, hence the inductance is virtually constant up to the maximum operating current. The inductance of a cell was determined from the measured pulse propagation, by the following procedure:

- Calculate flux by integrating, up to 350 ns, the potential difference between the two HV capacitance plates which sandwich the ferrite of the cell of interest;
- Divide the flux by the current flowing through resistor R_{out} at 350 ns; the current is calculated from the voltage drop across the resistor.

In order to improve the voltage resolution and the signal to noise ratio of the measured voltage, the magnitude of the driving signal was adjusted to be equal to the full-scale deflection of the Tektronix 11401 digitising oscilloscope utilised, and the signal was averaged 32 times. The same probe was used to measure both the voltage of each capacitance plate and across R_{out} . The measurement data was processed to remove the dc offset of the channel of the oscilloscope, and then normalised to the average of the voltage values in the time range of 350 ns to 500 ns. The normalisation process compensates for the drift of the Hewlett Packard 8082A pulse generator utilised for these measurements: the drift was measured to be approximately 0.06%. Special care was taken to ensure that the ground of the probe was always positioned adjacent to the midpoint of the back of the ground conductor, and the ‘live’ tip of the

probe was connected to the end of the leg of the HV capacitance plate. As a result of the procedure now adopted, these measurements are more accurate than those reported previously[4].

The self-inductance of the end cells was determined using two different procedures:

1. the ‘flat-top’ return current was allowed to flow through the ground striplines at the ends of the kicker;
2. the ‘flat-top’ return current was not permitted to flow through the ground striplines, but instead flowed through a wire which was arranged to have negligible mutual coupling to the end cell.

The measured inductance for each end cell of the prototype kicker, measured using the two methods (see above), is approximately 121 nH and 114.4 nH, respectively: thus 6.6 nH is attributable to mutual coupling between the ground stripline, at the end of the kicker, and the end cell. The self-inductance for the second and ninth cells is approximately 76 nH. The average cell inductance for the four central cells is 73.3 nH: the total self-inductance of the kicker, as determined from the two methods (see above) is 833 nH and 820 nH, respectively. The relative error between the measured inductances is estimated to be ± 1.9 nH, and the absolute error is estimated to be less than ± 2 %.

3 SIMULATIONS

Fringe fields result in an appreciable increase in inductance per cell towards the ends of the kicker. Hence in order to obtain realistic predictions it is necessary to employ a 3D code. In addition, because the excitation pulse contains high frequency components, it is important to model eddy currents: Elektra[6] is a 3D code which can simulate eddy currents.

Accurately simulating a magnet in 3D using a finite element code can require a large amount of memory and CPU time. In addition, the accurate simulation of eddy currents requires that there are an adequate number of finite elements per skin depth (e.g. 3), near to the surface of the conducting regions. However, due to symmetry of the kicker magnet, it is only necessary to model a quarter of the magnet (Fig. 2). Since displacement current is not simulated, it is not necessary to drive the model using a representative pulse: a representative pulse would require a significant number of finite elements in the conductors in order to accurately account for the eddy currents resulting from the Fourier spectrum of the pulse. Instead the model is excited using a sine-wave. The chosen frequency of the sine-wave (40 kHz) is high enough such that there is little magnetic field within the conductors: 40 kHz also corresponds to a frequency of interest for the LHC injection kickers[2].

The prototype kicker has striplines at its input and output. This kicker was designed to be driven from a matched impedance pulser, and terminated at its output using a matched resistive load. However the Elektra code does not permit external circuits to be modelled. The 3D model of

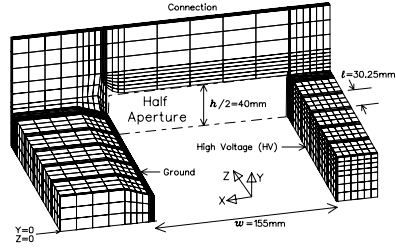


Figure 2: High voltage, ground and connecting conductor

the kicker magnet is driven from its centre: the HV conductor is connected to the ground conductor using the stripline of the end (ground) capacitance plate. Fig. 2 shows the HV, ground and connecting conductors simulated for the kicker magnet: for clarity the ferrite is omitted from the figure. In order to simplify the 3D model, the connection is represented as having the same shape as the ferrite cores. The two end HV capacitance plates, which sandwich the end ferrite, are omitted from Fig. 2: it is necessary to simulate these plates as they act as ‘eddy-current shields’ preventing magnet flux exiting through the side of the ferrites. Since the Y component of field is relatively constant within the 8 inner cells (see below) it is not necessary to simulate the HV capacitance plates, within the 8 inner cells, as conducting regions: it is sufficient to replace these HV capacitance plates by volumes of air, which also reduces the complexity of the model significantly.

The boundary condition set on the Y=0 plane enclosed between the HV, ground and connection is set to normal magnetic with a non-zero potential. The boundary condition on the Y=0 plane outside of the HV, ground and connection is set to normal magnetic with a zero potential. All non-conducting regions, except for the volume underneath the connecting conductor, are specified as being regions of total potential. The effect of the above is to set the net current enclosed (1 kA) by the contour integral around the HV and ground conductors to be equal to the value of the (non-zero) potential specified (see above). Similarly the volume underneath the connecting conductor is specified as being a region of non-conducting (air) vector potential: this ensures that the net current in the connection is equal to the specified potential.

The self-inductance of a cell towards the centre of the kicker can be estimated from the following equation:

$$L = \frac{\mu_0 \times w \times \ell}{h} \quad (1)$$

where, w is the width of the aperture (155 mm between the HV and ground); ℓ is the length of a cell (measured to be 30.25 mm) which is made up of ferrite (~ 25 mm) and a HV capacitance plate (~ 5 mm); and h is the height of the aperture (80 mm). Thus from equation 1, $L = 73.65$ nH.

The self-inductance of each inner cell is derived from the Elektra predictions by integrating the Y component of the predicted flux density (B_y) through the back yoke of the appropriate ferrite, along the Y=0 plane, and dividing the resultant flux by the total driving current. The predicted

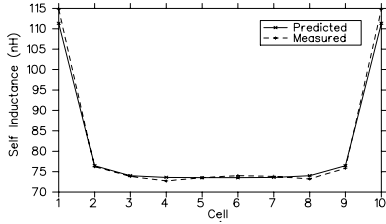


Figure 3: Predicted and measured cell self-inductance

inductance for the central cell is 73.54 nH, which is within 0.15% of that given by equation 1: the slight discrepancy is due to the fact that equation 1 treats the ferrite as having an infinite relative permeability, although this is somewhat offset by the fact that the aperture width of 155 mm neglects skin depth in the HV and ground conductors.

Calculating the self-inductance of the end cell by integrating B_y through the back yoke of the appropriate ferrite, along the $Y=0$ plane gives a value of 111.3 nH, in comparison with the 114.4 nH measured. The results file obtained from the Elektra simulation includes the total stored energy: this energy will include the mutual inductance between the end ground and HV striplines. Thus the predicted end-cell inductance was re-calculated by determining the total inductance (830 nH) from the stored energy, and subtracting the sum of the other cells inductance calculated from integrating B_y through the back yoke of the inner ferrites. The total predicted inductance (830 nH) is in excellent agreement with the measured total inductance (833 nH), and the calculated end-cell inductance is 120.6 nH. However, the HV and the ground striplines are modelled as having the same shape as the ferrites, so the predicted mutual inductance contribution may be slightly in error.

Fig. 3 shows the predicted self-inductance for each cell of the kicker. The end cells and second cells in from the end have an inductance 51% and 4% greater than the central cells, respectively. The measured self-inductance for each cell of the kicker is also shown in Fig. 3: there is good agreement between the measurements and predictions.

Omitting the end HV capacitance plate ('eddy-current shield') from the Elektra model results in the total predicted inductance for the kicker being 26 nH high: the self-inductance of each end cell and the second cell in from each end is increased by 12 nH and 1 nH, respectively. Omitting the HV capacitance plate between the two end ferrites does not modify the total predicted inductance for the kicker, however the distribution is modified such that the self-inductance of each end cell is reduced by 3 nH, and that of the second cell in from the end is increased by 3 nH.

Fig. 4 shows a plot of the predicted B_y along the centre of the aperture of the kicker. The predicted flux density is reasonably constant through the inner 8 cells of the magnet, but does start to decrease in value within the aperture of the second cell in from each end. At the end of the ferrite of the kicker magnet the flux density is approximately 73% of the value at the centre of the magnet. The flux density is 10% of the central value at a distance of approximately

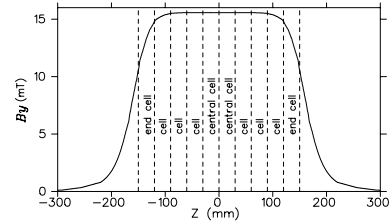


Figure 4: Y component of predicted flux-density

56 mm from the end of the ferrite.

The X and Y components of kick have been determined from $\int B_y \cdot dz$ and $\int B_x \cdot dz$, respectively. The effective length of the kicker (330 mm), at the centre of the aperture, is 9.2% greater than the actual length (302.5 mm). $\int B_y \cdot dz$, calculated from a 3D and 2D analysis, is within $\pm 1\%$ of the value at the centre of the aperture, for a fraction of the aperture area of approximately 0.69 and 0.79, respectively: the shape of the ferrite and conductors have previously been optimised with Opera2D[4].

4 CONCLUSION

Measurements carried out on a kicker magnet are in excellent agreement with predictions from the 3D eddy current code Elektra. Thus we are confident that Elektra can be successfully used to predict the inductance, field distribution and kick for the kicker magnets for LHC.

5 ACKNOWLEDGEMENT

The authors wish to acknowledge the useful technical discussions with present and former staff of the kicker magnet group of CERN PS Division. The authors would also like to thank staff of Vector Fields for their technical advice re the application of Elektra software to modelling of the kicker.

6 REFERENCES

- [1] Ducimetière L., Jansson U., Schröder G.H., Vossenber E.B., Barnes M.J. and Wait G.D., "Design of the Injection Kicker Magnet System for CERN's 14TeV Proton Collider LHC", Tenth IEEE International Pulsed Power Conference Albuquerque, June 1995.
- [2] Barnes M.J., Wait G.D., Ducimetière L., Jansson U., Schröder G.H., Vossenber E.B., "Kick Stability Analysis of the LHC Inflectors", Proceedings of this conference.
- [3] Fiander D., Metzmacher K., and Pearce P., "Kickers and Septa at the PS Complex", CERN. Proceedings of the KAON PDS Magnet Design Workshop, October 1988, pp71-79.
- [4] Wait G.D., Barnes M.J., Tran H.J., "Magnetic Field in a Prototype Kicker Magnet for the KAON Factory", IEEE Trans. on Magnetics, July 1994, Vol. 30, No. 4, pp2118-2121.
- [5] Barnes M.J., Wait G.D., "Kickers for the KAON Factory", Proceedings of the XVth International Conference on High Energy Accelerators, Hamburg, July 1992, pp194-196.
- [6] Vector Fields Inc., 1700 N. Farnsworth Avenue, Aurora, IL 60505. Tel. (708) 851 1734.